Original Paper

Hardness and flow behaviour of glass in the nanometre range – An interpretation of the load dependence of the hardness[1)]

Holger Meinhard, Peter Grau, Gunnar Berg and Susan Mosch

Fachbereich Physik, Martin-Luther-Universität Halle-Wittenberg, Halle (Germany)

The flow behaviour of glass was investigated by Vickers hardness indentation technique with variation of the deformation rate by six orders of magnitude. The hardness tests were carried out on commercial sheet glass with three different loading regimes. A general flow equation in form of a power law was used to describe the deformation behaviour of the materials. The influences of loading mode and deformation rate on the parameters of this law were investigated. An essential result of this work is that the load and penetration depth dependence of the hardness, respectively, the so-called indentation size effect, is an inevitability of the special methodology of the indentation technique during deformation of strain rate-sensitive materials.

Härte und Fließverhalten von Glas im Nanometerbereich – Deutung der Lastabhängigkeit der Härte

Das Fließverhalten von Glas wurde durch Vickershärte-Eindruckexperimente untersucht, bei denen die Deformationsrate über sechs Größenordnungen variiert wurde. Die Messungen wurden an kommerziellem Tafelglas mit drei verschiedenen Belastungsarten durchgeführt. Bei der Beschreibung des Materialverhaltens wurde von einer allgemeinen Fließgleichung in Form eines Potenzgesetzes ausgegangen. Der Einfluß der Belastungsart und der Belastungsgeschwindigkeit auf die Parameter dieses Gesetzes wurde untersucht. Wesentliches Ergebnis dieser Arbeit ist es, daß die Abhängigkeit der Härte von der Last und mithin von der Eindringtiefe eine notwendige Konsequenz der Methodik des Eindruckexperimentes bei der Verformung dehnungsratenempfindlicher Materialien ist.

1. Introduction

The mechanisms of permanent deformation of brittle glasses by scratching or point indentation close to room temperature have not been cleared up completely up to now. One of the suitable methods to investigate this problem is the recording hardness test. It is very important to clarify the special effects if this technique is to be employed.

The load and penetration depth dependence, respectively, the so-called Indentation Size Effect (ISE) [1], of the Vickers hardness has been a fundamental problem since measurements in the microrange ($F \leq 2N$) have been possible. Especially with modern equipment having resolution for the penetration depth in the nanometre range and for the applied force in the micro-Newton range, respectively, this behaviour is visible in a remarkable way.

ISE has been an object of many controversial discussions [2 and 3]. It is necessary to eliminate methodical uncertainties to identify this effect as a material behaviour. The influence of a possible indenter tip defect on hardness values was treated besides other things in [4]. A procedure was proposed in [5] to determine the zero points of load, indentation depth, and time scale as well as their accuracies, by extrapolation. The existence of ISE was shown unequivocally for glass, PMMA, and other materials even if all these influences were corrected.

The above investigations shall be continued in this paper. The ISE will be verified experimentally and derived theoretically from the special features of the indentation technique during deformation of strain rate-sensitive materials.

2. Fundamental assumptions and theoretical results

The possibility of nonreversible deformation of brittle glasses by indentation technique is associated with viscosity, plasticity and densification, respectively. But the last mentioned is negligible for sheet glass. It will be assumed as a fundamental hypothesis of this work that the time-dependent and strain rate-dependent deformation of glassy materials is determined by viscous flow. This statement is undisputed for deformation processes in the region above the transformation temperature (T_g). Then Newtonian flow determines the deformation of glass. This yields the relation

$$\sigma = m_D \eta_0 \dot{\varepsilon} \qquad (1)$$

where σ is the flow stress, $\dot{\varepsilon}$ the strain rate, η_0 the Newtonian viscosity and m_D the geometric constant of the

Received February 3, 1997.

[1)] Presented in German at: 70th Annual Meeting of the German Society of Glass Technology (DGG) on June 4, 1996 in Cottbus (Germany).

deformation process. The viscosity of glass is given by $\eta_0 = 10^{12.3}$ Pa s per definition at T_g, which corresponds to a relaxation time of $\tau \approx 100$ s. This can be used to estimate the typical strain rate $\dot{\varepsilon}$ caused by the contact pressure of the hardness tests $\sigma \approx H \approx 0.1\ G_\infty$, where H is the hardness and G_∞ is the modulus of rigidity, which depends on temperature only weakly. The relaxation time τ of Maxwellian type processes is given by

$$\tau = \frac{\eta_0}{G_\infty} \tag{2}$$

which yields with equation (1) a strain rate $\dot{\varepsilon} \approx 10^{-3}\ s^{-1}$. For room temperature a value of viscosity $\eta = 10^{20}$ Pa s or more was proposed, however, see e.g. [6]. This would lead to a relaxation time of about 100 years ($\tau \approx 10^{10}$ s) and a strain rate smaller than $\dot{\varepsilon} \approx 10^{-10}\ s^{-1}$ for the contact pressure in contradiction to the experience that hardness indentations can be realized on glass. Therefore, the flow law must be nonlinear for hardness tests to describe the behaviour of the materials adequately.

This can be fulfilled by the general flow law

$$\sigma = m_D\, b\, \dot{\varepsilon}^m \tag{3}$$

where b is the factor of viscosity and m is the exponent of the strain rate sensitivity. For $m = 1$ equation (3) stands for Newtonian flow behaviour and in this case $b = \eta_0$ is the Newtonian viscosity in accordance with equation (1). The flow behaviour of the material is inhomogeneous for $m < 1$ because of the location of the deformation in shear bands. These conditions exist for instance during deformation of solid glass cylinders near T_g [7], but they are also expected for hardness tests on glass at room temperature of course.

Equation (3) yields for hardness measurements

$$\sigma = m_D\, HU;\ \dot{\varepsilon} = \frac{\mathrm{d}h/\mathrm{d}t}{h} \tag{4}$$

where h is the indentation depth and HU the Universal Hardness [8], which is equal to the flow stress. Therefore, the strain rate $\dot{\varepsilon}$ decreases with increasing indentation depth characteristically for the penetration experiment. It will be shown that this behaviour has consequences for the depth dependence of the hardness. The indentation force is given as the resistance of the material to the penetration of the indenter in agreement with [9]. It yields [10]

$$F = k\, HU\, h^2 = k\, b \left(\frac{\dot{h}}{h}\right)^m h^2 \tag{5}$$

where F is the indentation force, k is the geometric constant of the indenter ($k = 26.43$ for Vickers pyramid), and $\dot{h} = \mathrm{d}h/\mathrm{d}t$ is the indentation rate. Three different loading regimes were used to prove equation (3) experimentally:

a) constant indentation rate (cir), with

$$\dot{h} = \dot{h}_c = \text{const} ; \tag{6a}$$

b) constant loading rate (clr), with

$$\dot{F} = \dot{F}_c = \text{const} ; \tag{6b}$$

c) variable indentation rate (vir) at constant piston speed $\dot{s}$ of a hydraulic material testing apparatus with a generalized form of equation (6a)

$$\dot{h} = \alpha \beta\, t^{\beta - 1},\ h = \alpha\, t^\beta . \tag{6c}$$

The experiments allow the measurement of the indentation force F dependent on indentation depth h and time t, respectively, as well as of the indentation depth h dependent on time t. All these relations were derived theoretically in [10] for the different loading regimes using equation (5) in connection with the equations (6a to c) for the experimental condition. It is an essential result that in all cases power laws were found:

$$F(h) = a\, h^n ; \tag{7a}$$

$$F(t) = a'\, t^{n'} ; \tag{7b}$$

$$h(t) = A\, t^B . \tag{7c}$$

With other words, the validity of the power law equation (3) for the strain rate dependence of the hardness leads inevitably to power laws of the different variables.

Equation (7a) is identical with the well-known Meyer law, which is often used to describe the ISE empirically. The so-called Meyer parameters n, n', B and a, a', A, respectively, of equations (7a to c) are determined by the parameters m and b of the flow law equation (3). The relations between these parameters are shown in table 1 as a result of the theoretical derivation in [10]. It is a remarkable result that the Meyer parameters depend on the loading regime, other than the material constants m and b which describe the real material behaviour only. Thus, it is not surprising that different authors using various loading regimes have measured different values of the Meyer parameters.

As mentioned the three variables F, h and t can be measured independently of one another for every loading regime. This gives the possibility of a consistency test with respect to the parameters determined empirically by equations (7a to c). The relations of table 2 follow directly from table 1, where the constants m and b were eliminated in the respective relations. Their fulfilment confirms on the one hand the applicability of the fundamental equation (3) and gives on the other hand an estimation of the zero point quality of the indentation force, the indentation depth and the test time scale, respectively. Additionally, all relations are given in table 2 to calculate the exponent m and the prefactor b of the fundamental flow law equation (3) by means of the experimental parameters, where the subscript h stands for the experimental indentation depth dependence and the

Table 1. Relations between parameters of Meyer's law and parameters of general flow law equation (3)

loading regime	$F = a h^n$	$F = a' t^{n'}$	$h = A t^B$
cir			
$\dot{h} = \dot{h}_c$	$n = 2 - m$	$n' = 2 - m$	$B = 1$
	$a = k b \dot{h}_c^m$	$a' = k b \dot{h}_c^2$	$A = \dot{h}_c$
clr			
$\dot{F} = \dot{F}_c$	$n = 2/(m+1)$	$n' = 1$	$B = (m+1)/2$
	$a = (k b)^{\frac{1}{m+1}} \left(\frac{m+1}{2} \dot{F}_c\right)^{\frac{m}{m+1}}$	$a' = \dot{F}_c$	$A = \left(\frac{\dot{F}_c}{k b}\right)^{1/2} \left(\frac{2}{m+1}\right)^{m/2}$
vir			
$\dot{h} = \alpha \beta t^{\beta-1}$	$n = 2 - m/\beta$	$n' = 2\beta - m$	$B = \beta$
	$a = k b \beta^m \alpha^{m/\beta}$	$a' = k b \beta^m \alpha^2$	$A = \alpha$

Table 2. Relations of consistency between the parameters of equations (7a to c)

loading regime	consistency	exponent m of flow law equation (3)	prefactor b of flow law equation (3)
cir			
$\dot{h} \equiv \dot{h}_c$	$n \equiv n'$	$m_h = 2 - n$	$b_h \equiv \frac{a}{k \dot{h}_c^m}$
	$a = \frac{a'}{\dot{h}_c^{n'}}$	$m_t = 2 - n'$	$b_t \equiv \frac{a'}{k \dot{h}_c^2}$
clr			
$\dot{F} = \dot{F}_c$	$n = \frac{n'}{B}$	$m_h = (2/n) - 1$	$b_h \equiv \frac{a^{m+1}}{k \left(\frac{m+1}{2} \dot{F}_c\right)^m}$
	$a = \frac{a'}{A^{n'/B}}$	$m_t = 2B - 1$	$b_t \equiv \frac{\dot{F}_c}{k A^2} \left(\frac{2}{m+1}\right)^m$
vir			
$\dot{h} = \alpha \beta t^{\beta-1}$	$n = n'/B$	$m_h = B(2 - n)$	$b_h \equiv \frac{a}{k B^m A^{m/B}}$
	$a = \frac{a'}{A^{n'/B}}$	$m_t = 2B - n'$	$b_t \equiv \frac{a'}{k B^m A^2}$

subscript t indicates the time dependence. The fulfilment of the conditions of consistency (table 2, column 2) automatically yields the equality $m_h = m_t$ for every case of the loading regime.

3. Experimental

The experiments with constant indentation rate (cir) and constant load rate (clr) were realized with the NANOINDENTER®II (Nano™ Instruments Inc., Oak Ridge, TN (USA)). Five different indentation rates (0.1 nm/s $\leq \dot{h}_c \leq$ 10 nm/s) were used for the cir test mode. The clr tests were realized for six different loading rates (1 mN/s $\leq \dot{F}_c \leq$ 50 mN/s) by reaching a maximum load F_{max} = 500 mN. All records of the single indentation experiments of these modes were analyzed from an indentation depth h_{lim} = 1 nm onward to exclude inaccuracies of data near the point where the indenter comes into contact with the sample.

The servohydraulic material testing system MTS 810 (MTS System Corporation, Minneapolis, MN (USA)) with an additional home-built equipment for hardness measurements was used to extend the range of the indentation rate. The vir tests were realized for fourteen different test piston speeds (1.7 nm/s $\leq \dot{s} \leq$ $\leq$ 33 333 nm/s), where a fixed maximum load F_{max} = = 2 N for all indentations were preselected. The data handling was done in agreement with the regulation of

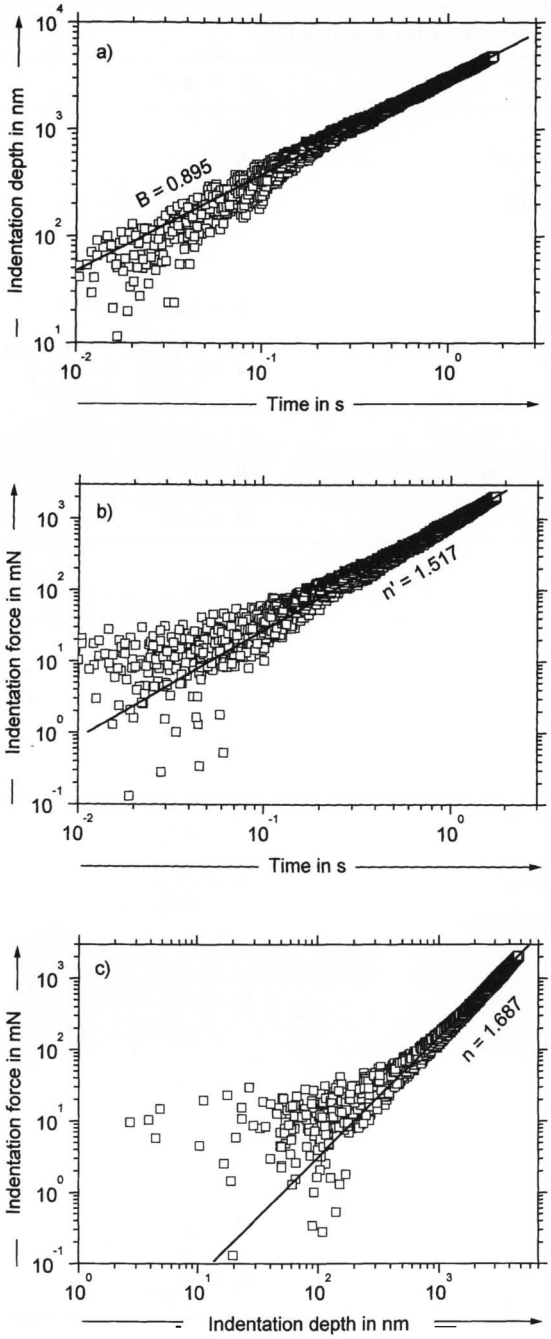

Figures 1a to c. Results of one of the vir tests with a constant piston speed of 3333 nm/s investigated by the hydraulic material testing system MTS 810. The slope of the straight part of the indentation depth versus time plot (figure a) is given by 0.895, which is equal to the parameter B of equation (7c) of this experimental condition. The slope of the straight part of the indentation force versus time plot (figure b) is given by 1.517, which is an example for calculation of parameter n' of equation (7b). The slope of the indentation force versus indentation depth plot (figure c) is given by 1.687, which is equal to the Meyer exponent n of equation (7a).

HU (see e.g. [8]). The oscillation of the data points of the measurements is more noticeable for MTS than for NANOINDENTER®II. The reason is the closed-loop control technique of servohydraulic testing systems.

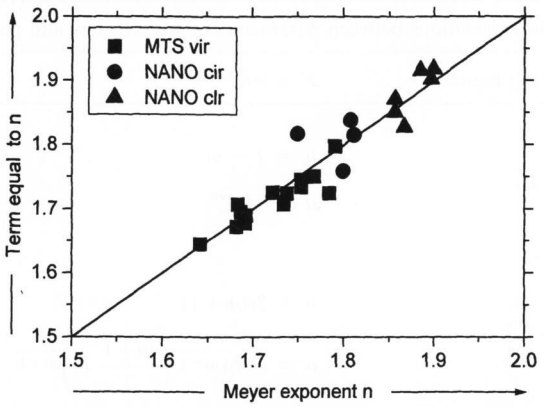

Figure 2. Representation of the consistency of the Meyer exponent n with the term equal to n in accordance with table 2 (column 2). Squares are originating from vir experiments (MTS), circles originate from cir experiments (NANO), and triangles are measured by clr experiments (NANO).

All experiments were performed on commercial sheet glass (composition (in mol%): 71 SiO_2, 15 Na_2O, 6.6 CaO, 4 MgO, 2 Al_2O_3, 0.9 K_2O, 0.4 SO_3, 0.1 Fe_2O_3) at room temperature and nearly 50% atmospheric humidity. The atmospheric humidity influences the viscosity of glass only sligthly [11 and 12]. For each of the 25 types of loading conditions ten single indentations were done. The values of all parameters were calculated for every single record and the arithmetic mean of the ten indentations with the same condition was determined.

4. Results and discussion

The experimental verification of the relations of consistency for every loading regime (see table 2) will be used to estimate the usability of the general flow law equation (3). It additionally gives an indication of accuracy of the description of the material behaviour during hardness measurements by this flow law. Figures 1a to c show the results of one of the vir tests as an example of the handling procedure. Lg-lg plots are used, because one expects power laws for all dependences. All data points of all single measurements are shown, the example with the highest variation of data points being selected intentionally. The slope of the straight line in the indentation depth versus test time plot in figure 1a gives the parameter $B = 0.895$ of equation (7c). The lg F-lg t plot of the same measurement is shown in figure 1b to enable the determination of the exponent $n' = 1.517$ of equation (7b). The Meyer exponent n of equation (7a) can be calculated directly as the slope of the straight line in the lg F-lg h plot in figure 1c. In this case the comparison of this Meyer exponent $n = 1.687$ with the quotient $n'/B = 1.695$ (see table 2, vir mode) clearly shows the good consistency.

This comparison for all experimental conditions is given in figure 2. The abscissa shows the real Meyer exponent determined from the $F(h)$ plot, where the ordi-

nate shows the term n'/B determined from the time dependences. The straight line indicates the ideal 1 : 1 correlation. The Meyer prefactor a, calculated from the same curves as the exponent n, is shown in figure 3 in a plot with the factor a calculated from a', A, n' and B originating from the experimental time dependences (see table 2). Also here the straight line gives the ideal 1:1 correlation.

A comparable way to check the consistency of the proposed analysis is the comparison of the parameters of equation (3) calculated by using the different dependences. The parameters m_h and m_t coincide consequently in accordance with the second and the third column of table 2. The parameters b_h and b_t show the analogous behaviour. By their excellent consistency all the results demonstrate the usability of the flow law equation (3) for a fixed loading regime.

The values of the exponent m of the flow law should not depend on the loading regime because its constancy as a material parameter was supposed during the analysis. The exponent m is shown for different deformation rates in figure 4, where solid and open symbols, respectively, indicate the different ways of the calculation of the values of m_h and m_t. They correlate excellently as also seen in figure 2 in accordance with columns 2 and 3 of table 2. But it must be clearly realized the difference of these parameters for various sets of the experimental arrangement (m_{vir} = 0.25, m_{cir} = 0.20, m_{clr} = 0.07, m_{creep} = 0.02). This result is a first hint of a certain shortcoming of the procedure. A similar phenomenon will be observed for the parameter of viscosity b. Its consistency within a special loading regime was already established above. But its representation for various loading regimes in a plot versus the strain rate in figure 5 shows two distinctive features. The prefactor b is an approximate constant for the clr mode, indeed, but it depends on the rate if loading regimes determined by the indentation rate are used. A change of six orders of magnitude causes a variation of the prefactor b of one order of magnitude. In addition, the various loading regimes yield different values of the parameters of viscosity.

But one should keep in mind that the flow law equation (3) is suitable to describe the depth dependence of the hardness on the whole, in spite of the mentioned inadequacies. Especially, it is taken into account that strongly varying experimental parameters were chosen very deliberately to test the supposition as far as possible. The consistency of the procedure could undoubtedly be shown for every loading regime. The different results comparing various loading regimes with one another and slight strain rate dependences of some parameters must be clarified in future work.

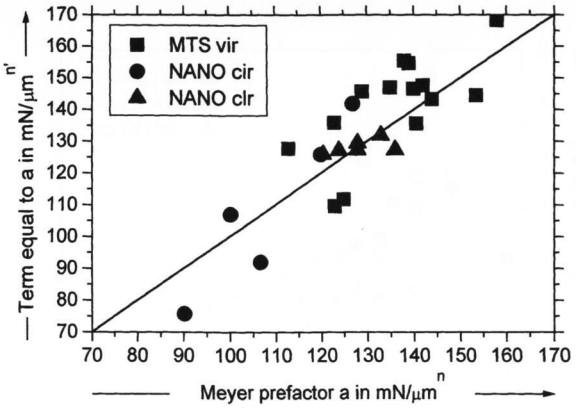

Figure 3. Representation of the consistency of the Meyer prefactor a with the term equal to a in accordance with table 2 (column 2). The different shapes of the symbols respresent the same loading regimes as in figure 2.

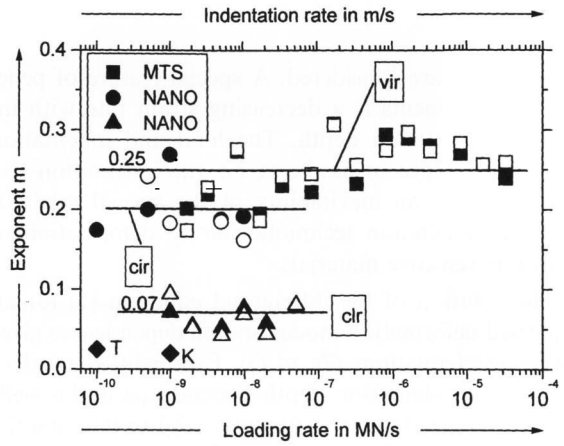

Figure 4. Exponents m of the general flow equation (3) in dependence on the deformation rate (indentation rate and loading rate, respectively). The different shapes of the symbols represent the same loading conditions as in figure 2. Solid symbols are calculated by indentation depth dependences and open symbols are calculated by the time dependences in accordance with table 2 (column 3). T and K denotes the results published in [11 and 12], respectively.

5. Summary and conclusions

The deformation behaviour of glass at room temperature was investigated by the modern universal hardness technique, where the simultaneous registration of indentation force, indentation depth, and test time is possible with high accuracy. Always hardness measurements are associated with nonreversible deformation. Newtonian flow determines the deformation of glassy materials in the region above the transformation temperature. But close to room temperature the mechanisms of permanent deformation of brittle glasses by indentation technique have not been cleared up completely up to now. It will be assumed as a fundamental hypothesis of this work that the process of deformation is determined by nonlinear viscous flow. For this reason, a general flow law (equation (3)) in form of a power law was used to describe this behaviour. A modification of equation (3) yields equation (5), where all measurable quantities of a

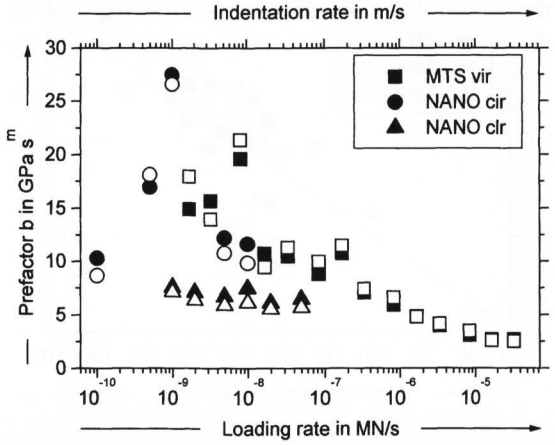

Figure 5. Prefactors b of the general flow equation (3) in dependence on the deformation rate. The nomenclature of the symbols is the same as in figure 4 (table 2, column 4).

hardness test are considered. A special feature of penetration experiments is a decreasing strain rate with increasing indentation depth. The load and indentation depth dependence of hardness, i.e. the indentation size effect (ISE), is an inevitability of the special methodology of indentation technique during deformation of strain rate-sensitive materials.

The solution of the differential equation (5) for all three used deformation modes and all dependences gives power laws (equations (7a to c)). Especially, the indentation force/indentation depth dependence is the well-known Meyer law, which often was used to describe the ISE empirically. All parameters of equations (7a to c) are determined by the parameters of the general flow law (table 1). This gives the possibility of a consistency test with respect to the relations of table 2, which follows directly from table 1. The results demonstrate an excellent consistency for all sets of experimental arrangements. So one can see the very good quality of the determination of the zero points of the indentation force, indentation depth and test time, respectively, using the procedure of calculation proposed in [5]. The applicability of the general flow law equation (3) is noticeable for fixed loading regimes at least, because the exponent m is independent of the deformation rate approximately. But it varies with different loading conditions. The parameter of viscosity b is an approximate constant for the clr loading mode. But the prefactor b becomes dependent on the rate for loading regimes determined by indentation rate (cir, vir).

The general flow law equation (3) was used also in [11 and 12], respectively, to investigate the influence of water in the surface of glassy samples. It was shown in [11 and 12] that different water contents do not cause significant differences of values of the exponent m. But it is very probable for physical reasons that water influences the flow behaviour of glass. Thus, only the viscosity factor b comes into question to depend on the water content. An investigation with regard to this problem will be a task of future work.

6. Nomenclature

6.1 Symbols

A	prefactor of the power law to describe the time dependence of the indentation depth
a	prefactor of Meyer's law
a'	prefactor of the power law to describe the time dependence of the indentation force
B	exponent of the power law to describe the time dependence of the indentation depth
b	factor of viscosity
F	indentation force
$\dot{F}$	loading rate ($=\mathrm{d}F/\mathrm{d}t$)
G_∞	modulus of rigidity
H	hardness
HU	universal hardness
h	indentation depth
$\dot{h}$	indentation rate ($=\mathrm{d}h/\mathrm{d}t$)
k	geometric constant of the indenter
m	exponent of the strain rate sensitivity
m_D	geometric constant of the deformation process
n	exponent of Meyer's law
n'	exponent of the power law to describe the time dependence of the indentation force
$\dot{s}$	piston speed of the hydraulic material testing system
T_g	transformation temperature
t	time
α	prefactor of the power law to describe the time dependence of the indentation depth if vir tests were used
β	exponent of the power law to describe the time dependence of the indentation depth if vir tests were used
$\dot{\varepsilon}$	strain rate ($=\dot{h}/h$)
η	viscosity
η_0	Newtonian viscosity
σ	flow stress
τ	relaxation time

6.2 Subscripts

c	constant
cir	constant indentation rate
clr	constant load rate
creep	indentation creep during constant load
h	calculated by indentation depth dependences
lim	limit
max	maximum
t	calculated by time dependences
vir	variable indentation rate

*

The authors thank the Deutsche Forschungsgemeinschaft, Bonn-Bad Godesberg, for sponsoring a part of this work under project no. Gr. 1482/1-1.

7. References

[1] Sargent, M. P.: Use of the indentation size effect on microhardness of materials characterisation. In: Blau, P. J.; Lawn, B. R. (eds.): Microindentation techniques in material science and engineering. In: ASTM STP 889. Philadelphia, PA: ASTM, 1986. p. 160–174.

[2] Bückle, H.: Mikrohärteprüfung und ihre Anwendung. Stuttgart: Berliner Union, 1965.
[3] Mott, B. W.: Micro-indentation hardness testing. London: Butterworth, 1956.
[4] Grau, P.; Berg, G.; Fränzel, W. et al.: Load dependence of the hardness of silicate glasses – Not just due to indenter tip defects. Glastech. Ber. **66** (1993) no. 12, p. 313–320.
[5] Grau, P.; Berg, G.; Fränzel, W. et al.: Recording hardness testing – Problems of measurements of small indentation depth. phys. stat. sol (a) **146**(1994) p. 537–548.
[6] Frischat, G. H.: Glas – Struktur und Eigenschaften. In: Lohmeyer, S.; Dannheim, H.; Frischat, G. H. et al.: Werkstoff Glas. I. 2. Aufl. Ehningen: expert Verl., 1987. p. 47–67.
[7] Brückner, R.; Yue, Y.; Habeck, A.: Determination of the rheological properties of high-viscous glass melts by the cylinder compression method. Glastech. Ber. Glass Sci. Technol. **67**(1994) no. 5, p. 114–129.
[8] Wehrstedt, A.: Übersicht über den Stand der Normung der Härteprüfverfahren für metallische Werkstoffe. VDI-Ber. **1194** (1995) p. 1–10.
[9] Martens, A.: Handbuch der Materialkunde für den Maschinenbau. Berlin: Springer, 1898.
[10] Grau, P.; Berg, G.; Meinhard, H. et al.: Strain rate dependence of hardness and Meyer's law. J. Am. Ceram. Soc. (In press.)
[11] Han, W.-T.; Tomozawa, M.: Indentation creep of $Na_2O \cdot 3SiO_2$ glasses with various water contents. J. Am. Ceram. Soc. **73** (1990) no. 12, p. 3626–3632.
[12] Keulen, N. M.: Indentation creep of hydrated soda–lime silicate glass determined by nanoindentation. J. Am. Ceram. Soc. **76** (1993) no. 4, p. 904–912.

1197P002

Address of the authors:

H. Meinhard, P. Grau, G. Berg, S. Mosch
Fachbereich Physik, Martin-Luther-Universität
Friedemann-Bach-Platz 6, D-06108 Halle